Powder Technology 201 (2010) 301–305

Contents lists available at ScienceDirect

Powder Technology

journal homepage: www.elsevier.com/locate/powtec

Short Communication

Kilogram-scale synthesis of Mg–Al–CO_3 LDHs nanosheets using a new two-stage reactor

Yue Jun Liu [a,*], Yong Sheng Que [a], Jun Yang [b], Ai Guo Yan [a]

[a] Key Laboratory of New Materials and Technology for Packaging, Hunan University of Technology, Zhuzhou 412007, PR China
[b] Zhuzhou Times New Material Technology Co., LTD, Zhuzhou 412007, PR China

ARTICLE INFO

Article history:
Received 10 December 2009
Received in revised form 7 March 2010
Accepted 24 March 2010
Available online 2 April 2010

Keywords:
Kilogram-scale synthesis
Mg–Al–CO_3–LDHs
Nanosheet
Two-stage reactor
Gas eddy
Liquid eddy

ABSTRACT

A novel reactor with a two-stage reaction chamber was designed to kilogram-large-scale synthesized Mg–Al–CO_3 layered double hydroxide (Mg–Al–CO_3 LDHs) nanosheets. The effects of the reactant concentration and rotation speed of the dynamic structure on the crystal size and morphology were investigated. The results show that the size of Mg–Al–CO_3 LDH particles gained in typical condition is about 50 nm in length and 5.7 nm in thickness, and the size becomes larger as the reactant concentration or rotationl speed decreased. The possible reaction mechanism was explained by three critical factors of the reactor, N_2 gas and polyethylene glycol 2000.

© 2010 Elsevier B.V. All rights reserved.

1. Introduction

Layered double hydroxide (LDH) nanomaterials have attracted extensive interests [1–3], because of their novel properties and extensive applications for catalysts [4], molecular container [5], flame retardants [6], and so on. Many methods for synthesizing LDH nanoparticles, including coprecipitation [7], ion exchange process [8], microwave synthesis [9], *etc.* have been developed. For these nanoparticles to be used, mass production is needed. Unfortunately, however, in most syntheses reported so far, gram-scale and small quantities of LDH nanoparticles were produced. So, large-scale synthetic approaches for nanoparticles (such as LDHs) remain a highly sophisticated challenge to materials scientists.

Reactor is a very important approach to prepare nanomaterials because it plays a role of executants to realize the reaction mechanism of chemistry or physical chemistry. In recent years, many researchers have designed different reactors to successfully synthesize nanocomposites. For example, Cafiero et al. [10] and Tai et al. [11] have used spinning disk reactors to prepare barium sulfate (a rotational speed higher than 900 rpm resulting in nanocrystals of 0.7 μm in averge size) and lamellar magnesium hydroxide (50–80 nm in length and 10 nm in thickness), respectively. However, these reactors lack a rapid mixing device, which results in the wide size distribution of the particles. Duan et al. [12] also invented a colloid mill to fabricate uniform magnesium hydroxide nanoparticles with a high degree of crystallinity. The theoretical basis of this approach is the LaMer model preparing monodisperse particles. However, the method is very complex and the entire reaction process lasts long time [13]. Thus, to design a reactor to realize rapidly mixing of different reagents and develop a simple preparation process is crucial to economical preparation of uniform nanoparticles.

The purpose of the experiment is to use a novel reactor to kilogram-scale synthesized Mg–Al–CO_3 LDH nanosheets and grope for new synthesis mechanism and fabrication processing of nanostructured materials.

2. Experimental sections

A schematic diagram of the reactor designed is shown in Fig. 1. It consists of liquid feeding systems (1, 10, and 12), dynamic structure (2, 4, 5, and 9), discharging systems (3, 13, and 18), and heat exchange systems (6, 16, and 17).

The chemical reaction involved in the formation of Mg–Al–CO_3 is as follows: Firstly, a molar ratio (2:1) of $MgCl_2 \cdot 6H_2O$ to $AlCl_3 \cdot 6H_2O$ was added into deionized water to form solution A. A certain amount of Na_2CO_3 ($[CO_3^{2-}] = 2.0[Al^{3+}]$), NaOH ($[OH^-] = 1.6[Mg^{2+} + Al^{3+}]$) and deionized water were mixed to make up solution B. A certain amount of surfactant such as polyethylene glycol 2000 (5–10 wt.% resulting product) and deionized water were mixed to form solution C. Secondly, at room temperature, the solutions A, B, C, and N_2 were pumped into the reaction chamber from feeding holes (10, left), (10, right), (12, left and right), and (1), respectively. Solutions A and B

* Corresponding author. Fax: +86 731 22622336.
E-mail address: yjliu_2005@126.com (Y.J. Liu).

0032-5910/$ – see front matter © 2010 Elsevier B.V. All rights reserved.
doi:10.1016/j.powtec.2010.03.026

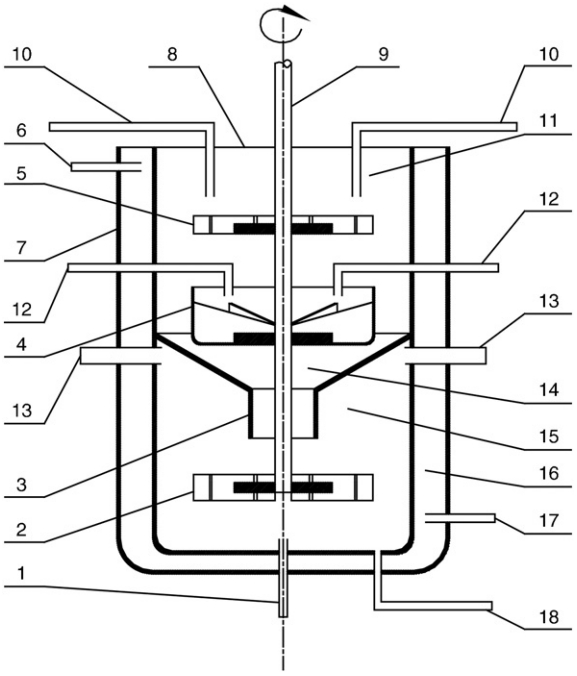

Fig. 1. The schematic diagram of the two-stage reactor: 1. gas intake, 2. agitator, 3. exit of reaction chamber I, 4. scattering groove, 5. impeller mixer, 6. exit of heat exchange chamber, 7. reactor shell, 8. reactor lid, 9. drive link, 10. feeding hole I, 11. reaction chamber I, 12. feeding hole II, 13. discharge hole I, 14. funnel-shaped reaction chamber inclined wall, 15. reaction chamber II, 16. heat exchange chamber, 17. entrance of heat exchange chamber, and 18. discharge hole II.

were quickly micromixed by twirling the impeller mixer (5) and gas eddy (Fig. 2). Meanwhile the mixture was thrown onto the inner wall of reaction chamber I to form large numbers of nucleus and then was rapidly coated by micro-droplets of surface agent coming from scattering groove (4). The suspension flowed onto the agitator (2) via exit of reaction chamber I (3) and was mixed adequately by gas eddy and liquid eddy in reaction chamber II (Fig. 2). After that, the slurry dynamically crystallized at 95–100 °C for 4–6 h. At last, the product was centrifuged (at 4500 rpm for 10 min), washed (with deionized water and 99.5% ethanol), dried (at 50–60 °C for 1 day), and milled (with a ceramic mortar) to obtain Mg–Al–CO_3 LDHs powder (2–5 kg, the productivity is about 0.4 kg/h).

Powder samples were analyzed with various techniques. X-ray powder diffraction (XRD) was performed on a D/MAX-III C automatic X-ray diffractometer with graphite-monochromatized Cu Kα radiation (V = 60Kv, I = 80 mA, scanning speed of 5°/min). The size and morphology of the particles were determined at 120 kV by JEM-1230 transmission electron microscope (TEM). The size distribution was determined by a Malvern Mastersizer 2000 laser particle size analyzer. Atom force microscopic (AFM) images were recorded by a Digital Instrument Nanoscope III Multimode system in tapping mode. A silicon cantilever with a bending spring constant of 20–60 N/m and a resonance frequency of about 250–350 kHz was used for imaging at a scan rate of 0.5–1.5 Hz.

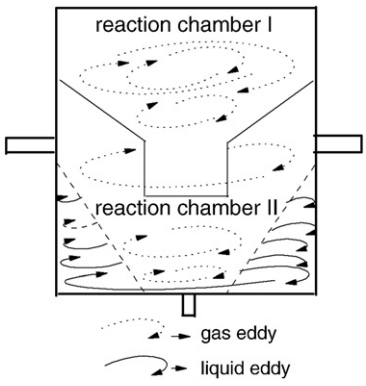

Fig. 2. The schematic diagram of distribution of gas eddy and liquid eddy in the reaction chamber, which basing on experimental observation, have two mass-transfer models, such as surface renew model [14], eddy cell model [15], and the fluid flow and mass transfer in a gas-injected vessel [16].

3. Results and discussion

Fig. 3A shows the typical SEM image of Mg–Al–CO_3 LDH nanosheets obtained and synthesized in the two-stage reaction chamber. It is indicated that the large quantity and good uniformity of Mg–Al–CO_3 LDH nanosheets were achieved by this approach. These nanosheets had a mean size of about 50 nm with good dispersion. The similar size was further observed by the typical TEM images of Mg–Al–CO_3 LDH nanosheets (Fig. 3B). Fig. 3C shows the typical XRD pattern of the as-prepared Mg–Al–CO_3 LDH nanosheets. All diffraction peaks in this pattern can be indexed as the pure hexagonal phase (JCPDS-14-191) [17]. No impurity peak was observed, which indicated that high purity crystalline Mg–Al–CO_3 LDHs were successfully synthesized by using this approach. As shown in Fig. 3D, the section analysis of the thickness of Mg–Al–CO_3 LDHs by AFM indicates that the thickness of the nanosheets is about 5.7 nm.

The phase structure and purity of the representative products were further characterized by X-ray powder diffraction (XRD). Fig. 4a, b, c, and d shows the XRD patterns of the samples synthesized at 1.6 M, 0.8 M, 0.4 M, and 0.2 M of molarities of [Mg^{2+}], respectively. The XRD patterns exhibit the characteristic reflections of Mg–Al–CO_3 LDH materials with a series of (00 l) peaks appearing as narrow symmetric lines at the low angle, corresponding to the basal spacing and higher order reflections [18]. The greater intensities and narrower line-widths of the peaks for Mg–Al–CO_3 LDHs indicate that, as previously reported [19]. Although the concentration of [Mg^{2+}] increased from 0.2 to 1.6 M, the XRD curves of Mg–Al–CO_3 LDHs have almost no change, which indicates that reaction concentration has little effect on the crystal structure.

TEM was also employed to further investigate the morphologies and structures of Mg–Al–CO_3 LDHs obtained. Fig. 5A is a TEM image of 35–40 nm crystals obtained at 1.6 M of [Mg^{2+}]. The inset in Fig. 5A is a higher magnification TEM image, from which it is clearly seen that nanocrystals are hexagonal nanosheets. The TEM image of the product obtained at 0.8 M of [Mg^{2+}] is shown in Fig. 5B and presents nanocrystals with the size of 40–50 nm. It is observed that there are some nanoparticles that appeared agglomerated slightly. Fig. 3C and D indicated that the size of the nanosheets increased (about 50–80 nm) when the molarity of [Mg^{2+}] decreased from 0.8 to 0.4 and 0.2 M, respectively. The possible reason is due to supersaturation, which plays the main role in controlling the mechanism and the kinetics of nucleation and growth processes. Especially very high level of supersaturation is required for homogeneous nucleation [10,20]. By increasing the reactants' concentration, the very high degree of supersaturation was generated, and the particles with smaller size and more regular morphology were obtained.

On the other side, we found that the rotation speed of the dynamic structure is also an extremely important factor to determine the size of particles. The experiments were carried out by changing the rotation speed and fixing the other operating variables. When the rotation speed was decreased from 1200 to 900 and 600 rpm, the mean size of Mg–Al–CO_3 LDH particles increased from ~5 nm (Fig. 6A) to ~60 nm (Fig. 6B) and ~80 nm (Fig. 6C), respectively. The laser particle analyzer was also employed to investigate the size distribution of the as-prepared samples (Fig. 6D and a, b and c indicate 1200, 900 and 600 rpm, respectively), which agree with the results of TEM well; the mean particle size and the diameter distribution of

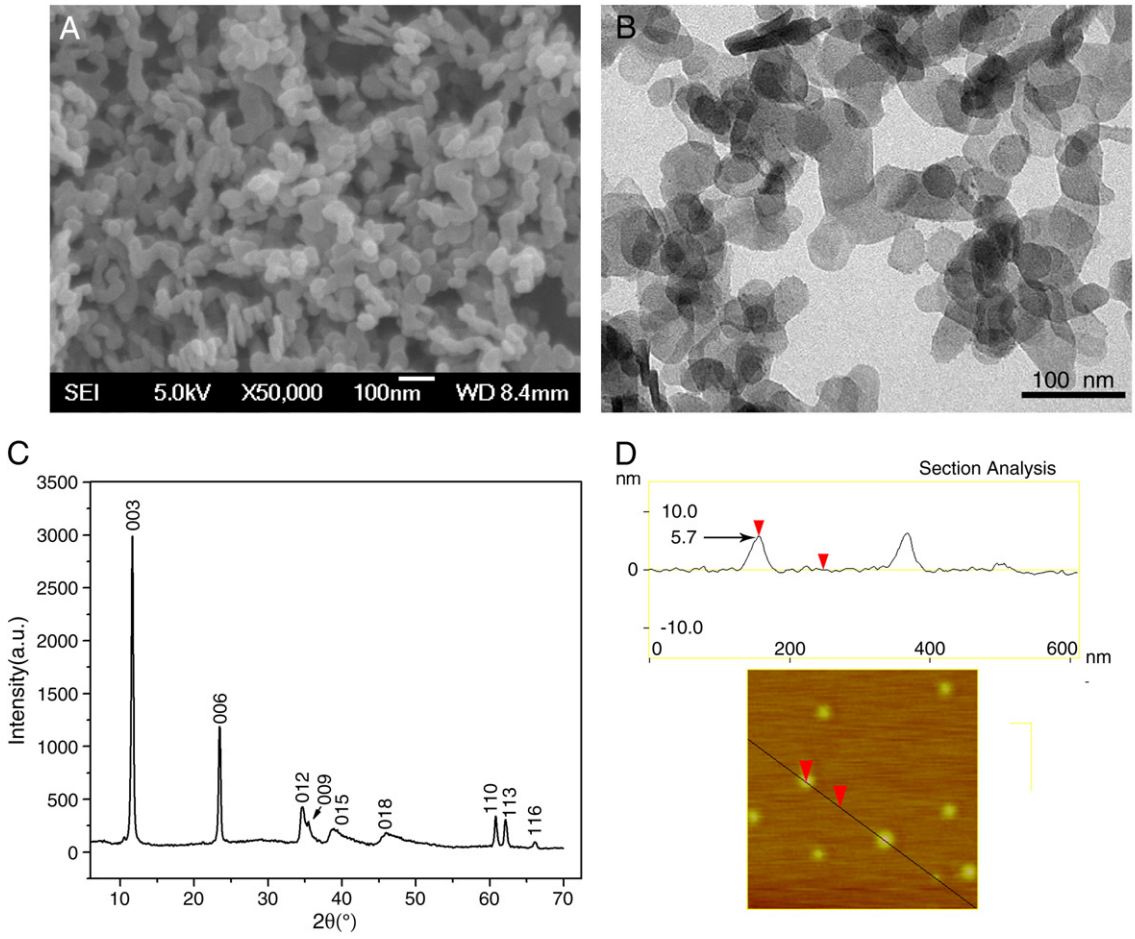

Fig. 3. (A) SEM image of Mg–Al–CO_3 LDH nanosheets synthesized in the two-stage reaction chamber and using polyethylene glycol 2000 as protective agent at 95 °C for 6 h. (B) TEM image of the same batch of sample. (C) XRD pattern of the same batch of sample. (D) Section analysis of AFM about thickness of Mg–Al–CO_3 LDHs.

Mg–Al–CO_3 LDH particles are smaller and narrower than the results reported respectively by Zhao et al. [18]. An increase of the rotation speed results in the reduction of particle size which is similar to the results reported by Cafiero et al. [10] and Tai et al. [11].

Moreover, the mechanism leading to the kilogram-scale synthesis of good uniformity Mg–Al–CO_3 LDH nanosheets by using a new two-stage reactor is not yet clear. However, our own experimental evidence has led us to believe that there are three key factors playing important roles in the formation of the lamellar Mg–Al–CO_3 LDH nanoparticles. Firstly, the new reactor separates crystal nucleation and growth steps by the two-stage reaction chamber (nucleation stage occurs mainly in reaction chamber I, and growth stage mainly performed in the reaction chamber II). Secondly, N_2 from the feeding hole (1) helps to form a great deal of gas eddy which further promotes mass transfer [14,15,21] and uniform particles [22]. Finally, the protective agent, polyethylene glycol 2000, prevents Mg–Al–CO_3 LDH nanosheets from congregating in the aging stage [23–25].

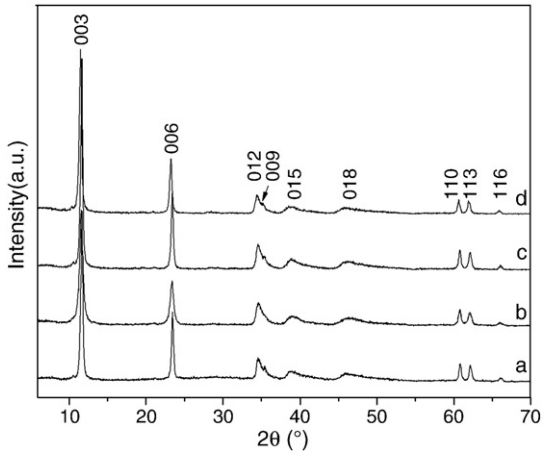

Fig. 4. XRD curves of Mg–Al–CO_3 LDH particles produced from different concentrations of [Mg^{2+}]. (a) 1.6 M, (b) 0.8 M, (c) 0.4 M, (d)0.2 M. [Mg^{2+}]/[Al^{3+}] = 2, L = 0.06 L/min, and N = 1200 rpm.

4. Conclusions

In this study, Mg–Al–CO_3 LDH nanosheets were successfully ultra-large-scale synthesized using a novel reactor with two reaction chambers. The results show that the size of the Mg–Al–CO_3 LDH particles obtained in a typical condition is about 50 nm in length and 5.704 nm in thickness, the size of the particles becomes larger as the reactant concentration or rotationl speed decreased. The possible reaction mechanism was explained basing on three critical factors: (1) the two-stage reactor separates crystal nucleation and growth steps; (2) N_2 from the feeding hole (1) helps to form a great deal of gas eddy; (3) polyethylene glycol 2000 prevents nanosheets from congregating in the aging stage. The deeper mechanisms will be further examined in future work.

Acknowledgments

Financial support of this work by the National Natural Science Foundation of China (No. 10672197 and No. 10972076), Outstanding

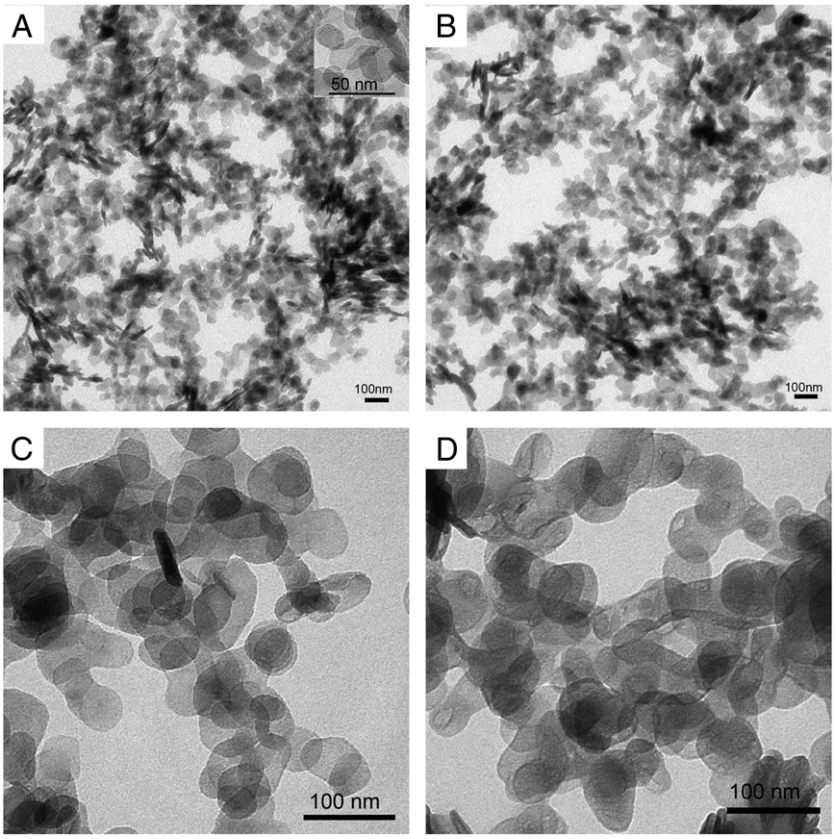

Fig. 5. TEM micrographs of Mg–Al–CO_3 LDH particles produced from different concentrations of [Mg^{2+}]: (A) 1.6 M, (B) 0.8 M, (C) 0.4 M, (D) 0.2 M; [Mg^{2+}]/ [Al^{3+}] = 2, L = 0.06 L/min, and N = 1200 rpm.

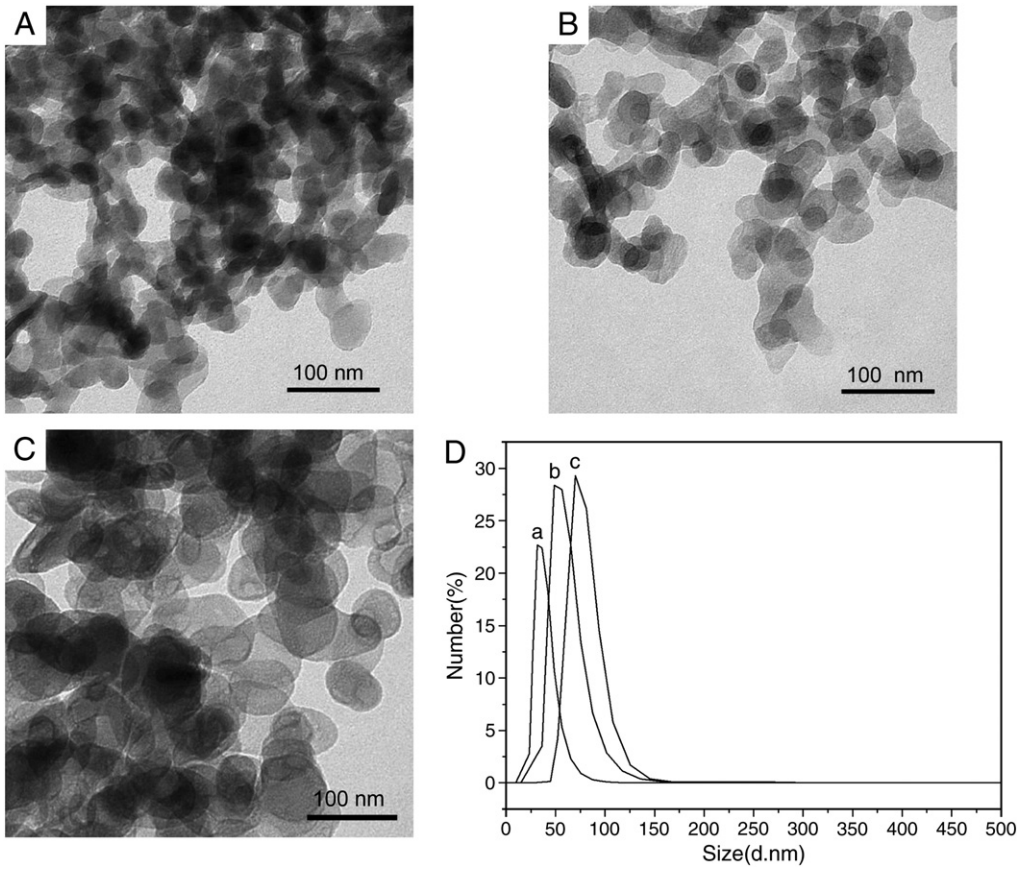

Fig. 6. TEM micrographs and profiles of particle diameter distribution of Mg–Al–CO_3 LDH particles produced under different rotational speeds and specific conditions at $L_1 = L_2$ = 0.06 L/min and N = 1200 rpm: (a) 1/1, (b) 3/4, (c) 1/2.

Youth Science Foundation of Hunan Province (No.07JJ1001), Technological Program of Hunan Province (No. 2009GK3127), and Graduate Innovation Foundation of Hunan Province (No.CX2009B199).

References

[1] J.S. Valente, F. Figureueras, M. Gravelle, J. Lopez, J.P. Besse, Basic properties of the mixed oxides obtained by thermal decomposition of hydrotalcites containing different metallic compositions, J. Catal. 189 (2000) 370–381.
[2] Y. Seida, Y. Nakano, Y. Nakamura, Crystallization of layered double hydroxides by ultrasound and the effect of crystal quality on their surface prooperties, Clays Clay Miner. 50 (2002) 525–532.
[3] M.J. Climent, A. Corma, S. Iborra, K. Epping, A. Velty, Increasing the basicity and catalytic activity of hydrotalcites by different synthesis procedures, J. Catal. 225 (2004) 316–326.
[4] C. Gerardin, D. Kostadinova, B. Coq, D. Tichit, LDH nanocomposites with different guest entities as precursors of supported Ni catalysts, Chem. Mater. 20 (2008) 2086–2094.
[5] Z.P. Xu, P.S. Braterman, High affinity of dodecylbenzene sulfonate for layered double hydroxide and resulting morphological changes, J. Phys. Chem. 13 (2003) 268–273.
[6] M.C. Costache, D. Wang, M.J. Heidecker, E. Manias, C.A. Wilkie, Polym. The thermal degradation of PMMA nanocomposites with montmorillonite, layered double hydroxides and carbon nanotubes, Adv. Technol. 17 (2006) 272–280.
[7] X. Duan, H. Zhang, R. Qi. WO2004009233Al29 Jan, (2004)15 pp.
[8] A.V. Radha, P. Vishnu Kamath, C. Shivakumara, Conservation of order, disorder, and "crystallinity" during anion-exchange reactions among layered double hydroxides (LDHs) of Zn with Al, J. Phys. Chem. B. 111 (2007) 3411–3418.
[9] M.Z.B. Hussein, Z. Zainal, Y.M. Chin, Microwave-assisted synthesis of Zn–Al-layered double hydroxide–sodium dodecyl sulfate nanocomposite, J.Mater. Sci. Lett. 19 (2000) 879–883.
[10] L.M. Cafiero, G. Baffi, A. Chianese, R.J. Jachuck, Process intensification: precipitation of barium sulfate using a spinning disk eactor, J. Ind. Eng. Chem. Res. 41 (2002) 5240–5246.
[11] C.Y. Tai, C.T. Tai, M.H. Chang, H.S. Liu, Synthesis of magnesium hydroxide and oxide nanoparticles using a spinning disk reactor, Ind. Eng. Chem. Res. 46 (2007) 5536–5541.
[12] X. Duan, Q. Jiao. Beijing University of Chemical Technology, Chinese patent (2000) 00132145.5.
[13] W.B. Zhang, B.H. Wang, W. Zhang, Preparation and applications of nanometer magnesium hydroxide, J. inorg. chem. ind. 36 (2004) 10–13 (in Chinese).
[14] P.V. Dankwerts, Significance of liquid-film coefficients in gas absorption, Ind. Eng. Chem. 43 (1951) 1460–1467.
[15] J.C. Lamont, D.S. Scott, An eddy cell model of mass transfer into the surface of a turbulent liquid, AIChEJ. 16 (1970) 513–519.
[16] T. Shoji, K. Seiji, K. Atsushi, Fluid flow and gas–liquid mass transfer in gas-injected vessels, Appl. Math. Model. 26 (2002) 249–262.
[17] U. Sharma, B. Tyagi, R.V. Jasra, Synthesis and characterization of Mg–Al–CO_3 layered double hydroxidefor CO_2 adsorption, Ind.Eng.Chem.Res. 47 (2008) 9588–9595.
[18] Y. Zhao, F. Li, R. Zhang, D.G. Evans, X. Duan, Preparation of layered double-hydroxide nanomaterials with a uniform crystallite size using a new method involving separate nucleation and aging steps, Chem. Mater. 14 (2002) 4286–4291.
[19] M.A. Pagano, C. Forano, J.P. Besse, Synthesis of Al-rich hydrotalcitelike compounds by using the urea hydrolysis reaction-control of size and morphology, J. Mater. Chem. 13 (2003) 1988–1993.
[20] J.L. Katz, Homogeneous nucleation theory and experiment: a survey, Pure&Appl. Chern. 64 (1992) 1661–1666.
[21] S. Goto, J. Levec, J.M. Smith, Mass transfer in packed beds with two-phase flow, Ind. Eng. Chem. Process Des. Dev. 14 (4) (1975) 473–478.
[22] C.L. Kitchens, C.B. Roberts, J.C. Liu, W.R. Ashurst, M.A. White, K.M. Hurst, S.R. Saunders, Application of gas-expanded liquids for nanoparticle processing: experiment and theory, Gas-Expanded Liquids and Near-Critical Media, 1006, 2009, pp. 290–308.
[23] P. Guha, D. Ganguli, S. Chaudhuri, Optical absorption of polyethylene glycol (PEG) modified silica matrix embedded with nanocrystalline silver, Mater. Lett. 58 (2004) 2963–2968.
[24] E. Esmaeili, A. Khodadadi, Y. Mortazavi, Microwave-induced combustion process variables for MgO nanoparticle synthesis using polyethylene glycol and sorbitol, J. Eur. Ceram. Soc. 29 (2009) 1061–1068.
[25] M. Sertkol, Y. Köseoğlu, A. Baykal, H. Kavas, A.C. Basaran, Synthesis and magnetic characterization of $Zn_{0.6}Ni_{0.4}Fe_2O_4$ nanoparticles via a polyethylene glycol-assisted hydrothermal route, J. Magn. Magn. Mater. 321 (2009) 157–162.